BIOCHEMISTRY

Articles

b_6f-Associated Chlorophyll: Structural and Dynamic Contribution to the Different Cytochrome Functions[†]

Agnès de Lacroix de Lavalette,[‡] Giovanni Finazzi,[§] and Francesca Zito*,[‡]

UMR 7099, CNRS and Université Paris-7, and UMR 7141, CNRS and Université Paris-6, Institut de Biologie Physico-Chimique, 13 rue Pierre et Marie Curie, F-75005 Paris, France

Received January 31, 2008; Revised Manuscript Received March 21, 2008

ABSTRACT: Cytochromes bc_1/b_6f complexes catalyze electron transfer from lipid- to water-soluble carriers in both the respiratory and photosynthetic processes. They contain several common redox cofactors, while a chlorophyll *a* molecule, the function of which is still enigmatic, is only present in b_6f-type complexes. In this work, we describe a mutagenesis approach aimed at characterizing the role of this pigment. Mutants of the binding pocket were constructed to obtain cytochrome (cyt) b_6f complexes altered in chlorophyll position and/or stability. On the basis of a combined biochemical and functional analysis, we conclude that the chlorophyll plays a major structural role in the complex. Moreover, the chlorophyll and its binding pocket may also be implicated in the regulation of photosynthetic state transitions, a function that is specific to cyt b_6f complexes.

Cytochrome (cyt) b_6f complex is a central component of the photosynthetic chain, which transfers electrons from Photosystem (PS)II[1] to PSI. It comprises four major subunits as well as several minor subunits of small molecular weight (*1*).

In addition, cyt b_6f contains one molecule of chlorophyll *a* (Chl*a*) and one of β-carotene per monomer (*2–7*). The functional role of these pigments is still debated (see refs *3–5* and *8* for discussions). Previous studies have shown

that the chlorophyll molecule is an intrinsic component of the cyt b_6f complex (*2, 3, 8, 9*) and that it may sense the electron transfer at the Q_o site (*10*). The recent X-ray structures of complexes from the chlorophyte *Chlamydomonas reinhardtii* (*8*) and the cyanobacterium *Mastigocladus laminosus* (*9*) have provided a rationale for these results. While the chlorine ring of Chl*a* is sandwiched between helices F and G of the subunit IV, where it may exert a structural role, the phytyl chain protrudes into the entrance of the hydroquinone oxidizing site, Q_o. There, it likely comes in contact with PQ/PQH$_2$ (see ref *8*) and may therefore sense its presence and position during the catalytic cycle of the complex.

Besides its role in electron transfer from plastoquinol to plastocyanin, cyt b_6f plays another critical function in photosynthesis, by triggering state transitions. This term describes a mechanism whereby photosynthetic organisms balance the supply of excitons between the two photosystems (*11–15*). Transition from state 1 to state 2 results from the transfer of a

fraction of the outer PSII light-harvesting complex (LHCII) to PSI, a process triggered by the phosphorylation of LHCII (*16*). During a state 2 → state 1 transition, LHCII is dephosphorylated and reassociates with PSII (*12*). Modulation of the phosphorylation state of antenna proteins results from the opposite actions of a LHCII−kinase, the activation of which is redox-dependent (*17*), and a phosphatase, which is generally considered to be permanently active (*18*). Kinase activation requires a reduced plastoquinone pool, as well as an active cyt b_6f complex (*13, 17, 19, 20*). Data obtained *in vitro* (*21, 22*) as well as *in vivo* with *C. reinhardtii* (*13, 23*) indicate that the first step in kinase activation is the binding of plastoquinol to the Q_o site of the b_6f complex. This generates an activating signal, which is then transduced from the luminal site of the membrane, where the Q_o site is located, to the stromal site, where LHCII phosphorylation takes place (e.g., see refs *15* and *24* for reviews).

A possible role for the chlorophyll in this process has been proposed on the basis of the observation that the tetrapyrrole ring of the chlorophyll molecule is exposed to the lipid phase, while its phytyl chain points toward the Q_o site, allowing a possible interaction with the plastoquinone (*8, 25*). Consequently, the chlorophyll molecule may provide a pathway that signals the presence of a quinol in the Q_o site to the peripheral region of the complex, where kinase docking might take place.

The aim of this work was to modify the chlorophyll environment to gain information on the role of this molecule. We used a site-directed mutagenesis approach to modify the native Chl*a* binding site by introducing bulky amino acids. Dependent upon the position of the modified residue, this results in a more or less pronounced slowing down of cyt b_6f turnover, as well as a reduced stability of the dimeric form *in vitro* and a loss of the Chl*a* molecule from its binding site. Furthermore, a significant decrease in the state 1 to state 2 transition rate is observed in some of the mutants, reinforcing the hypothesis that the chlorophyll may play a direct or indirect role in the process of kinase activation.

MATERIALS AND METHODS

Strains, Media, and Growth Conditions. Δ*petD* (mt+) deletion strain (*26*) was used as a recipient strain in chloroplast transformation experiments, and FCterH$_6$ strain (mt+) (H$_6$F$_5$), histidine-tagged (*27*), was used as a control strain. H$_6$F$_5$ and mutant strains were grown on Tris−acetate−phosphate (TAP) medium (pH 7.2) at 25 °C under dim light (5−6 μE m^{-2} s^{-1}).

Plasmids, Oligonucleotides, and Mutagenesis. The plasmid carrying the entire sequence of *petD* and the C-terminal histidine tag of cyt *f* was obtained as follows. Plasmid pFWH$_6$ (*8*) was digested with *Eco*RV and *Acc*I, and the 0.55 kb fragment was ligated at the corresponding sites in the pdWQ (*26*), yielding plasmid pWQH$_6$.

Plasmid encoding the mutant *petD* was created by polymerase chain reaction (PCR)-mediated site-directed mutagenesis. To generate the mutation in positions 104 and 136 of the *petD* gene, plasmid pdΔHI.I (*26*), carrying the entire coding sequence of *petD*, was used as a template in PCR reactions using as primers the following oligonucleotides:

V$_{104}$F$_{dir}$, 5′-GGG**CCTAGG**TGTATTATTAATGGCAG-CA**TTC**CCTGCAGGCCTTATCACGGT-3′

V$_{104}$F$_{rev}$, 5′-GGG**CCTAGG**AGTTTGTTTGGAACTA-CACGTAAA-3′

V$_{136}$F$_{dir}$, 5′-GGG*GACGTC*CAATCGCTACTATCTTAT-TCCTTTTA**TTC**ACTTTAGTTGCTGTTTGTTAG-3′

V$_{136}$F$_{rev}$, 5′-GGG*GACGTC*GGTATGGGTTTTGGAA-3′.

Arrow Taq DNA polymerase was employed according to the instructions of the manufacturer. The PCR product was digested with *Avr*II for the 104 mutation (bold in the sequence) and with *Aat*II for the 136 mutation (italic in the sequence) and religated onto themselves to yield plasmids pdΔHV104F and pdΔHG136F, respectively. The double mutant V$_{104}$-G$_{136}$F was obtained using the plasmid pdΔHV104F as a template for PCR, with oligonucleotides V$_{136}$F$_{dir}$ and V$_{136}$F$_{rev}$ yielding plasmid pdΔHV104-G136F carrying both restriction sites *Avr*II and *Aat*II.

These three plasmids were digested with *Hin*dIII and *Nco*I, and the 833 bp fragment was ligated at the corresponding sites in the plasmid pWQH$_6$, yielding plasmids pdV104F, pdG136F, and pdV104F-G136F.

Chloroplast Transformation in C. reinhardtii. The *petD* strain, bearing a deletion of the *petD* gene was transformed by tungsten particle bombardment according to ref *28* with plasmids pdV104F, pdG136F, and pdV104F-G136F. Transformants were selected on minimum medium at 60μE m^{-2} s^{-1}.

Preparative and Analytical Techniques. Cells grown to a density of 4×10^6 mL^{-1} were broken in "bead-beater" (Biospec-Products) according to the instructions of the manufacturer. The membrane fraction was collected by centrifugation and resuspended in 10 mM Tricine at pH 8 at a chlorophyll concentration of 3 g L^{-1}. For sodium dodecyl sulfate−polyacrylamide gel electrophoresis (SDS−PAGE), membrane proteins were resuspended in 100 mM dithiothreitol and 100 mM Na$_2$CO$_3$ and solubilized by 2% SDS at 100 °C for 1 min. Polypeptides were separated on a 12−18% polyacrylamide gel containing 8 M urea. Immunoblotting was performed as described in ref *2*. Cyt b_6f complexes were isolated as described in ref *8*. Electron-transfer activity measurements on the purified complexes were performed as described in ref *2*. Cyt b_6f complexes were analyzed by size-exclusion chromatography in 20 mM Tris-HCl at pH 8.0, 250 mM NaCl, and 0.2 mM C$_{12}$M onto an exclusion HR200 Amersham column (*6*).

In Vivo Phosphorylation of Antenna Proteins. Cells grown at 3×10^6 cells mL^{-1} were harvested and resuspended in a phosphate-depleted medium containing 1 μCi mL^{-1} ^{33}P$_i$. Then, they were treated as described in ref *29*.

Fluorescence Measurements. Fluorescence measurements were performed at room temperature on a home-built fluorimeter, using a light source at 520 nm. The fluorescence response was detected in the near IR region. Fluorescence spectra at 77 K were recorded using a home-built spectrophotometer based on a detecting diode array (AVS-USB 200, Ocean Optics, Dunedin, FL). Samples were loaded on a small metal cuvette (volume ∼ 15 μL), which was directly immersed into the liquid nitrogen bath. Excitation was provided by a LED source [peak at 470 nm, full width at half maximum (FWHM) ∼20 nm], which was directed to the sample through an optical guide.

Absorption Spectroscopy. Time-resolved light-induced absorbance changes in whole cells of *C. reinhardtii* were monitored with a pulsed differential LED spectrophotometer
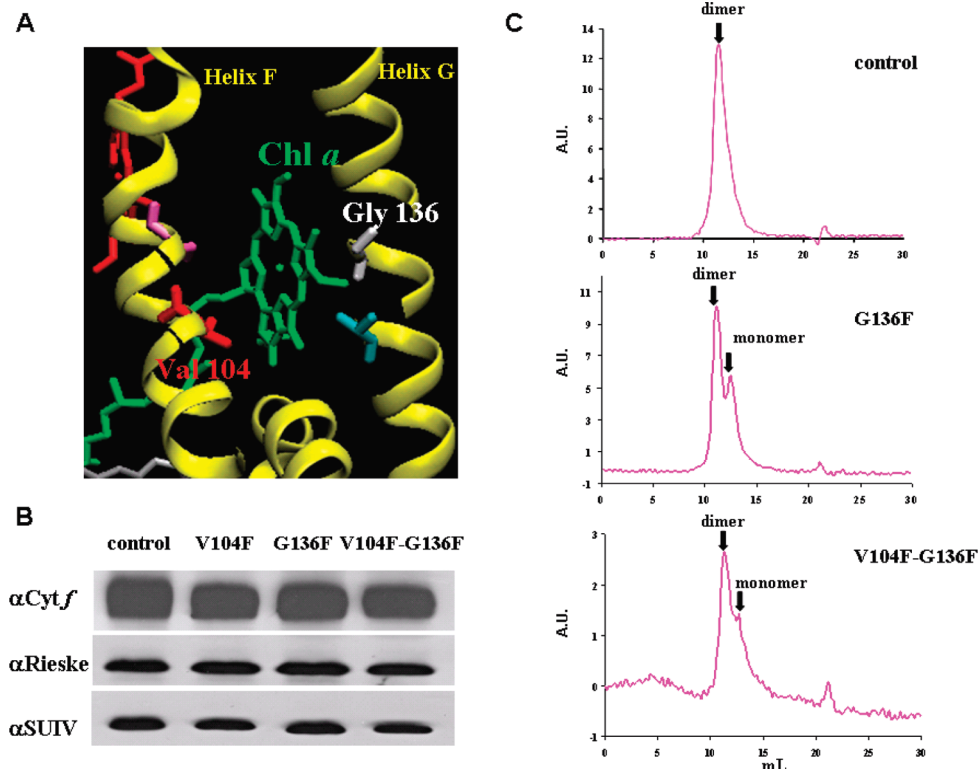
FIGURE 1: Biochemical characterization of cyt b_6f complex mutants. (A) Chl*a* binding site in the cyt b_6f complex from *C. reinhardtii*. (B) Immunoblot of membrane protein extracts probed with specific antibodies against cyt *f*, Rieske protein, and subunit IV. Loads for each sample correspond to 20 μg of chlorophyll. (C) Size-exclusion chromatography analysis of the WT and G136F and V104F-G136F mutant b_6f complexes. Samples (100 μL) were analyzed on a 10 × 300 mm Superdex 200 HR column. The absorbance of the eluate was monitored at 280 nm.

(JTS10, Biologic, France) as originally described in ref *30*. The transmembrane potential was estimated by the amplitude of the electrochromic shift at 520 nm, which yields a linear response with respect to the electric component of the transmembrane potential (*31*). Under the conditions employed here, the kinetics of the electrochromic signal displayed two phases previously described in ref *32*: a fast phase completed in less than 1 μs, associated with PSI and PSII charge separation (phase a), and a slow phase, which develops in the millisecond time range, associated with the turnover of the cyt b_6f complex (b phase). Cyt *f* redox changes were evaluated as the difference between absorption at 554 nm and a baseline drawn between 545 and 573 nm. A small correction for the contribution of the electrochromic signals (5% of the signal observed at 515 nm) was made.

RESULTS

Construction of C. reinhardtii Mutants. The role of the Chl*a* molecule in the structure/function of the cyt b_6f complex was investigated by site-directed mutagenesis. According to the crystallographic structure of the complex, the chlorine ring of the chlorophyll molecule is sandwiched between helices F and G of subunit IV and faces a valine at position 104 and a glycine at position 136 (Figure 1A). Either one or both of these amino acids were substituted by bulkier residues, such as a phenylalanine.

Phototrophic clones were recovered from a transformation of $\Delta petD$ strain with plasmids pdV104F, pdG136F, or pdV104F-G136F. All of them display growth rates comparable to that of the wild type (WT) in both photoautotrophic and myxoautotrophic conditions. Furthermore, they do not show any photosensitivity in high light (550 μE, data not shown).

In Vitro Characterization. All mutants accumulated the major subunits of the cyt b_6f complex at about the WT levels (Figure 1B). In particular, the content in SUIV, which harbors the mutations, was unaltered. The characteristics of the different strains are summarized in Table 1; the absorption spectrum of the cyt b_6f-associated chlorophyll is red-shifted in the mutants, with the most pronounced effect being observed in the G136F strain, and their Chl*a*/cyt*f* ratio is decreased. The shift in the Chl*a* peak is accompanied by a decreased rate of electron transfer *in vitro*, which is reduced by a factor of 2, 5, and 18 in the V104F, V104F-G136F, and G136F mutants, respectively. The oligomerization state of the cyt b_6f complex, as measured by size-exclusion chromatography, is also affected by some of the mutations (Figure 1C). While a single peak can be observed in the WT (Figure 1C) as well as in the V104F (not shown), two peaks appear in the G136F mutant: the first one at 12 mL, which corresponds to the dimer, and the second one at 13 mL, which corresponds to the monomer. A similar tendency is seen in the double mutant, where however, the yield of the monomer is much more limited than in the G136 strain (Figure 1C).

In Vivo Electron-Transfer Activity. The catalytic cycle of cyt b_6f comprises oxidation of PQH$_2$ at the Q$_o$ site of the protein complex and reduction of PQ at the Q$_i$ site. According to the "Q cycle" (*33, 34*), PQH$_2$ oxidation allows for injection of electrons into two distinct paths: one comprising the Rieske protein and cyt *f* (the "high-potential" chain) and the

Table 1: Characteristics on WT and Mutant Purified Cyt b_6f [a]

mutant	dimer	Chl$a$/cyt f	Chl$a$ peak (nm)	activity e^-/b_6f/s	state transitions amplitude	state transitions $t_{1/2}$ (min)
control	+++	1.2	667	~400	0.30 ± 0.03	5 ± 1.1
V104F	+++	0.6	669	~220	0.35 ± 0.02	5 ± 1.0
G136F	+	0.5	675	~25	0.24 ± 0.01	10 ± 0.9
V104F-G136F	++	0.1	672	~80	0.25 ± 0.04	11 ± 1.4

[a] Dimerization is assessed according to the elution profile, as shown in Figure 1. The chlorophyll absorption maximum of the Q_y band is measured in isolated cyt b_6f preparations, which were also used to assess electron flow activity as in ref *2*. State transitions amplitude and $t_{1/2}$ refer to an average of at least 10 experiments realized over several months ± standard error. These parameters (amplitude and $t_{1/2}$) were evaluated from a fit of traces as in Figure 2 with a single-exponential decay function.

Table 2: Relevant Photosynthetic Parameters of WT and Mutant Cells *in Vivo* [a]

mutant	b phase $t_{1/2}$ (ms)	cyt f re-reduction $t_{1/2}$ (ms)
control	3 ± 1	3 ± 1
V104F	3 ± 2	3 ± 1.5
G136F	9 ± 4.5	11 ± 2.2
V104F-G136F	12 ± 2	11 ± 1.4

[a] The b phase was measured in the presence of 1 μM FCCP to remove any kinetic limitation by light-induced acidification of the lumen (e.g., see ref *43*).

other involving the two b_6 hemes (the "low-potential" chain). The catalytic cycle can be studied spectroscopically by either measuring the redox changes of cyt f (*35*) or following the kinetics of the transmembrane potential rise in the millisecond time range ("b phase" of the electrochromic signal; see refs *32* and *36*).

In vivo, the G136F and V104F-G136F mutants displayed a significant decrease of the electron-transfer rate as compared to the WT. While the $t_{1/2}$ of cyt f re-reduction and the b phase was ~3 ms in the WT, it increased to around 10−12 ms in the G136F and V104-G136F mutants. The V104F mutant showed no differences when compared to the control (Table 2).

State Transitions in the Simple and Double Mutants. We next monitored the occurrence of state transitions in the mutant strains by measuring the fluorescence yield at room temperature in the presence of the PSII inhibitor 3-(3,4-dichlorophenyl)-1,1-dimethylurea (DCMU) (*14*). When PSII photochemistry is inhibited, it is possible to follow directly the changes in its antenna size by measuring the extent of the fluorescence signal (*37*). Mutants were placed in conditions that promote either state 1 (dark and strong agitation) or state 2 [5 μM carbonylcyanide-4-(trifluoromethoxy)-phenylhydrazone (FCCP) in the dark] in the control strain, and their fluorescence yield was monitored. About 20 min are required before maximal quenching of fluorescence (witnessing the completion of state 2 transitions) could be observed in the WT (parts A and B of Figure 2) and the V104F mutant (not shown). This transition was clearly slower in both the G136F mutant (parts A and B of Figure 2 and Table 1) and the V104F-G136F double mutant (not shown). The occurrence of state transitions in the mutants is confirmed by the increased relative contribution of PSI fluorescence under state 2 conditions, when measured at cryogenic temperature (Figure 2C) and by assessing the time course of protein phosphorylation in the different strains by a protein phosphorylation essay (Figure 3); cells were preincubated for 90 min with $^{33}P_i$ and placed for 20 min in state 1 and 2 conditions in a $^{33}P_i$-free medium as previously described (*13*).
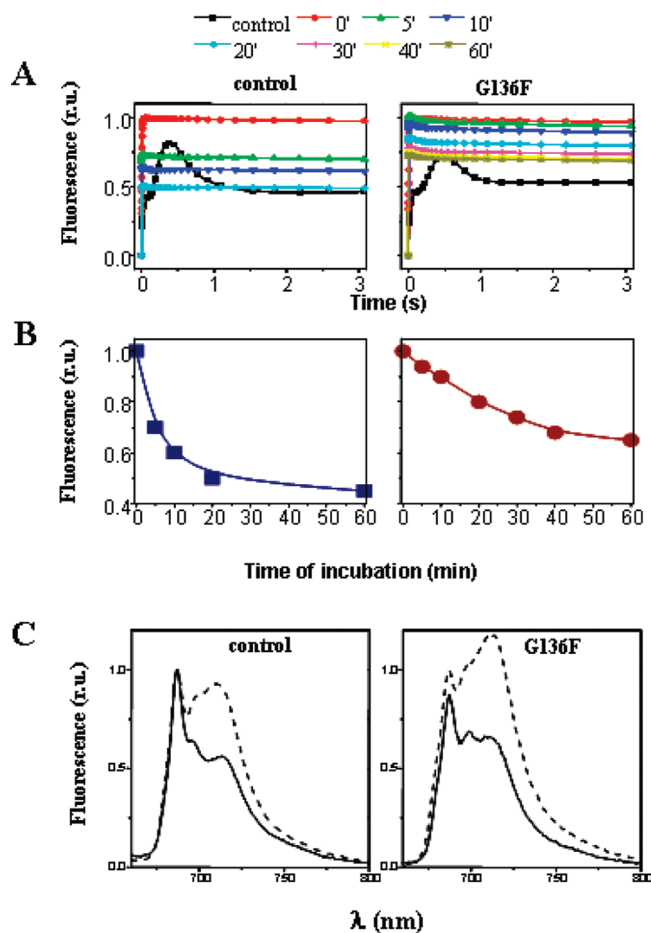

FIGURE 2: State transitions in WT and G136F mutant strains. (A) Fluorescence yield at room temperature in the presence of 10 μM DCMU. WT and G136F mutant were placed in either state 1 (darkness under strong aeration, red curve) or state 2 (darkness in the presence of 5 μM FCCP) conditions. Black, control; red, DCMU added; green, DCMU added 5 min; blue, DCMU added 10 min; cyan, DCMU added 20 min; magenta, DCMU added 30 min; yellow, DCMU added 40 min; and brown, DCMU added 60 min. (B) Decay of the fluorescence yield in WT and G136F mutant. (C) Contribution of PSII and PSI fluorescence under state 1 and 2 conditions at 77 K.

The phosphorylation profiles of thylakoid membrane polypeptides from WT and the G136F mutant display a similar labeling pattern. However, while in the WT, the phosphorylation of LHCII polypeptides, LHC-P13 and LHC-P17, is complete after 10 min, it takes ~30 min in the mutant. Interestingly, the same delay in protein phosphorylation is also observed in the case of the minor phosphoproteins that were detected in the 15−20 kDa region, including the cyt b_6f-associated protein PetO, which likely represents the first protein to be phosphorylated upon kinase activation, even
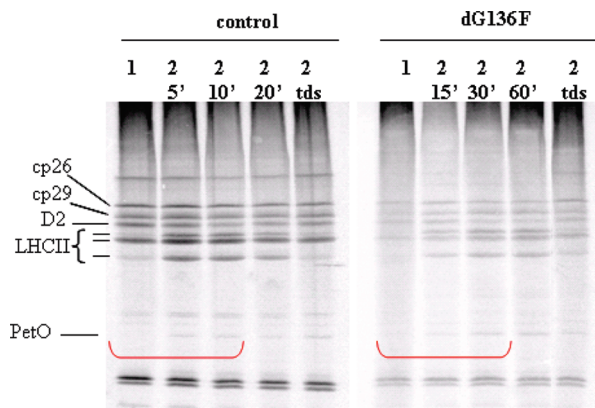
FIGURE 3: Autoradiogram of ^{33}P-radiolabeled antenna polypeptides in the 25−35 kD region. Cells were placed in state 1 and state 2 conditions and state 2 plus tridecylstigmatellin (tds). The same sample and conditions are used for fluorescence measurements as in Figure 2.

in the presence of trydecilstigmatellin, an inhibitor of the Q_o site (lane tds in Figure 3) (*23, 38*). Thus, it appears that the slowing down of state transitions in the mutant reflects a slower activation of the LHCII kinase by the cyt b_6f complex.

DISCUSSION

In this work, we address the question of the possible role(s) of chlorophyll molecule associates with the cyt b_6f complex by comparing the structural and functional properties of different strains generated by site-directed mutagenesis. The rationale was to modify the chlorophyll environment, by replacing the native amino acids facing the chlorophyll ring with bulkier residues. The observed results (Figure 2 and Table 1) are consistent with the view that the main role of the chlorophyll is to provide a structural bridge between helices F and G of subunit IV (*8*), which may compensate for the lack of the additional helix, which occupies a similar location in the homologous respiratory complex, cyt bc_1 (*39, 40*).

We show that the replacement of the glycine in position 136 of SUIV with a phenylalanine favors the release of the chlorophyll from the complex as well as the monomerization of the latter. No such effect is seen upon replacing the valine in position 104 with the same bulky residue. In this case, the mutated complex behaves very similarly to its WT counterpart. Analysis of the 3D structure of the cyt b_6f complex likely provides an explanation for these contrasting phenotypes. While both the valine and the glycine face the chlorophyll ring (Figure 1), the Chl*a* pocket is sufficiently large to accommodate a phenylalanine in position 104. On the other hand, the presence of the phytyl chain probably imposes a major steric constraint, which accounts for the conservation of a small residue (glycine) at position 136 in the WT. This probably explains for the stronger phenotype associated with this mutation. Interestingly, an intermediate phenotype is seen when both mutations are combined; the V104F-G136F mutant complex purifies as a stable and relatively active dimer, although its overall chlorophyll content is drastically decreased, being reduced to ∼10% of the WT content. *In vivo*, this mutant displays a very similar slowing down in electron transfer as the dG136F mutant (Table 2) and in the state transitions capacity (Table 1),

despite the different stability of their complexes upon purification (see Figure 1). Thus, we conclude that both the overall rate of electron flow and the state transitions capacity are poorly related to the monomerization tendency *in vitro*.

Again, an analysis of our data in light of the 3D structure of the complex may provide an explanation for these results. The position of the Chl*a* molecule suggests that it likely plays a structural role, by providing a bridge between helices F and G of subunit IV. Thus, the introduction of a bulky amino acid in position 136 may result in a strong rearrangement of the site, as indicated by the strong shift in the absorption spectrum of the chlorophyll molecule. On the other hand, the simultaneous introduction of a second mutation (V104F) may result in the recovery of the initial conformation. This may well occur via the exclusion of the Chl*a* from its pocket (as indicated by the finding that the [Chl]/[cyt *f*] ratio drops to 0.1, i.e., a value very close to the one associated with the presence of contaminating chlorophyll in the complex) and its replacement by the two phenylalanines. Thus, the concomitant presence of two bulky residues may fill the chlorophyll pocket and provide a stability element, even in the absence of this pigment.

The most striking feature of the chlorophyll mutants analyzed here is the slowing down of state transitions (Table 1). It seems unlikely that this effect could be a direct consequence of the reduced efficiency of the electron flow process. Indeed, previous studies on *C. reinhardtii* have shown that an impaired electron transfer is usually not accompanied by a state transitions phenotype (*41−43*).

As an alternative possibility, we consider the hypothesis that a modification of the structure in the vicinity of the chlorophyll environment may affect the process of activation of the kinase. This process involves several partners, namely, cyt b_6f, the light-harvesting complex, and the LHCII kinase. According to our previous model for LHCII kinase activation (*14*), the interaction between the kinase and the cyt b_6f complex is a critical step in state transitions. It requires an "active" cytochrome complex, capable of switching between the docking conformation, which activates the kinase, and a releasing one, where the active kinase becomes capable of interacting with LHCII. This model is based on the finding that phosphorylation of the cyt b_6f-linked protein PetO (*15, 23, 38*) can occur even when the enzymatic activity of the complex is blocked by adding a specific plastoquinone analogue, tridecylstigmatellin. This inhibitor seems to block the cytochrome in its "docking" conformation (*23, 44, 45*), because no further phosphorylation of LHCII is seen in its presence (*15*).

With regard to this hypothesis, it is tempting to speculate that the chlorophyll mutants may show a slower rate of state transitions because of a decreased capacity to dock the kinase. What is the rationale behind this suggestion? A similar behavior (i.e., a blockade of state transitions in a mutant with no impairment of the electron flow capacity) has been already observed in a chimeric mutant, in which an extra copy of the minor subunit PetL was fused to the C terminus of helix G of SUIV. In this case, the data were interpreted in terms of a correct docking of the kinase by the "active" cytochrome complex being precluded because of the presence of an extra helix close to docking site (*14*). That same helix G of SUIV is involved, together with helix F, in sandwiching the chlorophyll molecule. Thus, it is reasonable to assume that
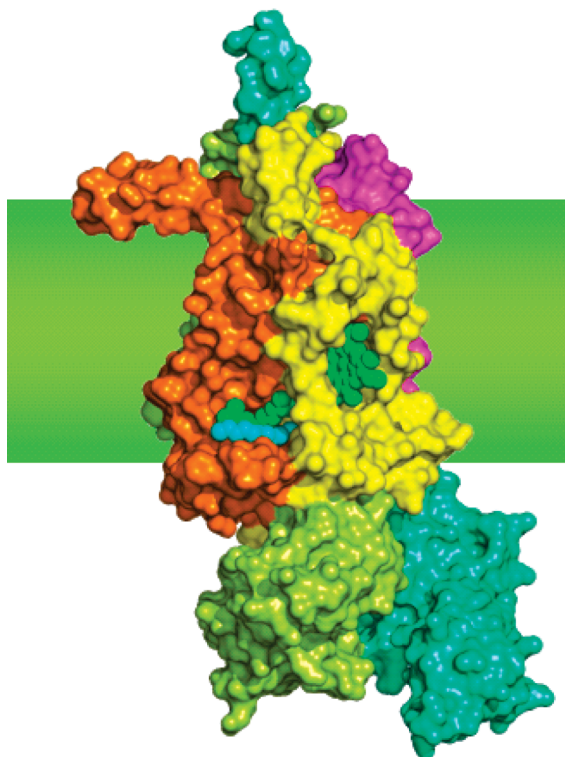
FIGURE 4: Location and interactions of Chl*a* with respect to subunits and other cofactors in the cyt b_6f complex from *C. reinhardtii*. (A) Space-filling model of Chl*a* in its environment (side view). Green, Chl*a*; cyan, tridecylstigmatellin; yellow, subunit IV; orange, cyt b_6; lime, Rieske; light blue, cyt *f*; and magenta, small subunits. Note the van der Waals contact between the phytyl tail of the Chl*a* and the alkyl chain of tridecylstigmatellin. This figure was based on crystallographic data from ref *8* [Protein Data Bank (PDB) file 1Q90] and realized with the PyMOL Molecular Graphics System.

the docking site for the LHCII kinase in the cyt b_6f may encompass the chlorophyll-binding domain. The structure of the cytochrome complex shows that this chlorophyll-binding pocket has a convenient location/position (Figure 4A) for kinase docking, because it is at the interface with the membrane and exposed to the lipidic phase. It can be speculated therefore that, while the docking site had been masked in the chimera mutant by the fused PetL subunit, the structural changes induced in the chlorophyll mutants may partially modify this site, owing to structural rearrangements in the cytochrome complex.

Alternatively, a different possibility has to be considered, in which the chlorophyll-binding site may not directly participate in the docking of the kinase. In this case, it is still possible to account for the reduced rate of state 2 transition in the mutants, considering that the phytyl chain, which is in contact with the plastoquinol-binding site (Figure 4), may provide the transducing element that detects the presence and/or the location of plastoquinol in the Q_o site (as required for kinase activation) and transmits it to the stromal catalytic part of the kinase. In the frame of this second hypothesis, it is worth noting that a concomitant increase in the rate of both electron flow and state transitions has been observed during time evolution of one clone of the G136F mutant (de Lacroix de Lavalette and Zito, unpublished results). The existence of a tight link between the rates of cyt b_6f turnover and state transitions reinforces the hypothesis that the role of the chlorophyll in modulating the

state transition is mainly to transduce a Q_o-site-generated signal rather than to provide a docking site. Further work is in progress to distinguish between these two not necessarily mutually exclusive hypotheses.

REFERENCES

1. Cramer, W. A., Soriano, G. M., Ponomarev, M., Huang, D., Zhang, H., Martinez, S. E., and Smith, J. L. (1996) Some new structural aspects and old controversies concerning the cytochrome b_6f complex of oxygenic photosynthesis. *Annu. Rev. Plant Physiol. Plant Mol. Biol. 47*, 477–508.
2. Pierre, Y., Breyton, C., Kramer, D., and Popot, J.-L. (1995) Purification and characterisation of the cytochrome b_6f complex of *Chlamydomonas reinhardtii*. *J. Biol. Chem. 49*, 29342–29349.
3. Pierre, Y., Breyton, C., Lemoine, Y., Robert, B., Vernotte, C., and Popot, J.-L. (1997) On the presence and role of a molecule of chlorophyll *a* in the cytochrome b_6f complex. *J. Biol. Chem. 272*, 21901–21908.
4. Pierre, Y., Chabaud, E., Herve, P., Zito, F., and Popot, J.-L. (2003) Site-directed photochemical coupling of cytochrome b_6f-associated chlorophyll. *Biochemistry 42*, 1031–1041.
5. Zhang, H., Huang, D., and Cramer, W. A. (1999) Stoichiometrically bound β-carotene in the cytochrome b_6f complex of oxygenic photosynthesis protects against oxygen damage. *J. Biol. Chem. 274*, 1581–1587.
6. Huang, D., Everly, R. M., Cheng, R. H., Heymann, J. B., Schagger, H., Sled, V., Ohnishi, T., Baker, T. S., and Cramer, W. A. (1994) Characterization of the chloroplast cytochrome b_6f complex as a structural and functional dimer. *Biochemistry 33*, 4401–4409.
7. Cramer, W. A., Yan, J., Zhang, H., Kurisu, G., and Smith, J. L. (2005) Structure of the cytochrome b_6f complex: New prosthetic groups, Q-space, and the "hors d'oeuvres hypothesis" for assembly of the complex. *Photosynth. Res. 85*, 133–143.
8. Stroebel, D., Choquet, Y., Popot, J.-L., and Picot, D. (2003) An atypical haem in the cytochrome b_6f complex. *Nature 426*, 413–418.
9. Kurisu, G., Zhang, H., Smith, J. L., and Cramer, W. A. (2003) Structure of the cytochrome b_6f complex of oxygenic photosynthesis: Tuning the cavity. *Science 302*, 1009–1014.
10. Joliot, A., and Joliot, P. (1995) In *Photosynthesis: From Light to Biosphere* (Mathis, P., Ed.) pp 615−618, Kluwer Academic Publishers, Dordrecht, The Netherlands.
11. Bonaventura, C., and Myers, J. (1969) Fluorescence and oxygen evolution from *Chlorella pyrenoidosa*. *Biochim. Biophys. Acta 189*, 366–383.
12. Allen, J. F. (1992) Protein phosphorylation in regulation of photosynthesis. *Biochim. Biophys. Acta 1098*, 275–335.
13. Zito, F., Finazzi, G., Delosme, R., Nitschke, P., Picot, D., and Wollman, F.-A. (1999) The Q_o site of cytochrome b_6f complexes controls the activation of the LHCII kinase. *EMBO J. 18*, 2961–2969.
14. Zito, F., Vinh, J., Popot, J.-L., and Finazzi, G. (2002) Chimeric fusions of subunit IV and PetL in the b_6f complex of *Chlamydomonas reinhardtii*: Structural implications and consequences on state transitions. *J. Biol. Chem. 277*, 12446–12455.
15. Wollman, F. A. (2001) State transitions reveal the dynamics and flexibility of the photosynthetic apparatus. *EMBO J. 20*, 3623–3630.
16. Bennett, J. (1991) Protein phosphorylation in green plant chloroplasts. *Annu. Rev. Plant Physiol. Plant Mol. Biol. 42*, 281–311.
17. Allen, J. F., Bennett, J., Steinback, K. E., and Arntzen, C. J. (1981) Chloroplast protein phosphorylation couples plastochinone redox state to distribution of excitation energy between photosystems. *Nature 291*, 25–29.
18. Elich, T. D., Edelman, M., and Mattoo, A. K. (1997) Evidence for light-dependent and light-independent protein dephosphorylation in chloroplasts. *FEBS Lett. 411*, 236–238.

19. Horton, P., and Black, M. T. (1981) Light-dependent quenching of chlorophyll fluorescence in pea chloroplasts induced by adenosine 5′-triphosphate. *Biochim. Biophys. Acta 635*, 53–62.

20. Wollman, F.-A., and Lemaire, C. (1988) Studies on kinase-controlled state transitions in photosystem II and *b₆f* mutants from *Chlamydomonas reinhardtii* which lack quinone-binding proteins. *Biochim. Biophys. Acta 85*, 85–94.

21. Vener, A. V., Van Kan, P. J., Gal, A., Andersson, B., and Ohad, I. (1995) Activation/deactivation cycle of redox-controlled thylakoid protein phosphorylation. Role of plastoquinol bound to the reduced cytochrome *b₆f* complex. *J. Biol. Chem. 270*, 25225–25232.

22. Vener, A. V., Van Kan, P. J., Rich, P. R., Ohad, I., and Andersson, B. (1997) Plastoquinol at the quinol oxidation site of reduced cytochrome bf mediates signal trasduction between light and protein phosphorylation: Thylakoid protein kinase deactivation by a single turnover flash. *Proc. Natl. Acad. Sci. U.S.A. 94*, 1585–1590.

23. Finazzi, G., Zito, F., Barbagallo, R. P., and Wollman, F. A. (2001) Contrasted effects of inhibitors of cytochrome *b₆f* complex on state transitions in *Chlamydomonas reinhardtii*. The role of Q_o site occupancy in LHCII kinaes activation. *J. Biol. Chem. 276*, 9770–9774.

24. Rochaix, J. D. (2007) Role of thylakoid protein kinases in photosynthetic acclimation. *FEBS Lett. 581*, 2768–2775.

25. Finazzi, G. (2005) The central role of the green alga *Chlamydomonas reinhardtii* in revealing the mechanism of state transitions. *J. Exp. Bot. 56*, 383–388.

26. Kuras, R., and Wollman, F.-A. (1994) The assembly of cytochrome *b₆f* complexes: An approach using genetic transformation of the green alga *Chlamydomonas reinhardtii*. *EMBO J. 13*, 1019–1027.

27. Choquet, Y., Zito, F., Wostrikoff, K., and Wollman, F. A. (2003) Cytochrome *f* translation in *Chlamydomonas* chloroplast is autoregulated by its carboxyl-terminal domain. *Plant Cell 15*, 1443–1454.

28. Boynton, J. E., Gillham, N. W., Harris, E. H., Hosler, J. P., Johnson, A. M., Jones, A. R., Randolph-Anderson, B. L., Robertson, D., Klein, T. M., and Shark, K. B. (1988) Chloroplast transformation in *Chlamydomonas* with high velocity microprojectiles. *Science 240*, 1534–1538.

29. Wollman, F. A., and Delepelaire, P. (1984) Correlation between changes in light energy distribution and changes in thylakoid membrane polypeptide phosphorylation in *Chlamydomonas reinhardtii*. *J. Cell Biol. 98*, 1–7.

30. Joliot, P., and Joliot, A. (1988) The low-potential electron transfer chain in the cytochrome *b/f* complex. *Biochim. Biophys. Acta 933*, 319–333.

31. Witt, H. T. (1979) Energy conversion in the functional membrane of photosynthesis. Analysis by light pulse and electric pulse methods. *Biochim. Biophys. Acta 505*, 355–427.

32. Joliot, P., and Delosme, R. (1974) Flash-induced 519 nm absorption change in green algae. *Biochim. Biophys. Acta 357*, 267–284.

33. Mitchell, P. (1975) Protonmotive redox mechanisms of the cytochrome *bc₁* complex in the respiratory chain: Protonmotive ubiquinone cycle. *FEBS Lett. 56*, 1–6.

34. Crofts, A. R., Meinhardt, S. W., Jones, K. R., and Snozzi, M. (1983) The role of the quinone pool in the cyclic electron-transfer chain of *Rhodopseudomonas sphaeroides*: A modified Q-cycle mechanism. *Biochim. Biophys. Acta 723*, 202–218.

35. Joliot, P., Béal, D., and Delosme, R. (1998) In vivo measurments of photosynthetic activity: Methods, in *The Molecular Biology of Chloroplasts and Mitochondria in Chlamydomonas* (Rochaix, J.-D., Goldschmidt-Clermont, M., and Merchant, S., Eds.) pp 433−449, Springer Publishing, New York.

36. Joliot, P., and Joliot, A. (1994) Mechanism of electron transfer in the cytochrome *b/f* complex of algae: Evidence for a semiquinone cycle. *Proc. Natl. Acad. Sci. U.S.A. 91*, 1034–1038.

37. Butler, W. L. (1978) Energy distribution in the photochemical apparatus of photosynthesis. *Annu. Rev. Plant Physiol. Plant Mol. Biol. 29*, 345–378.

38. Hamel, P., Olive, J., Pierre, Y., Wollman, F. A., and de Vitry, C. (2001) A new subunit of cytochrome *b₆f* complex undergoes reversible phosphorylation upon state transition. *J. Biol. Chem. 275*, 17072–17079.

39. Soriano, G. M., Ponamarev, M. V., Carrell, C. J., Xia, D., Smith, J. L., and Cramer, W. A. (1999) Comparison of the cytochrome *bc₁* complex with the anticipated structure of the cytochrome *b₆f* complex: Le plus ca change le plus c'est la meme chose. *J. Bioenerg. Biomembr. 31*, 201–213.

40. Berry, E. A., Guergova-Kuras, M., Huang, L., and Crofts, A. R. (2000) Structure and function of cytochrome *bc* complexes. *Annu. Rev. Biochem. 69*, 1005–1075.

41. Yan, J., and Cramer, W. A. (2003) Functional insensitivity of the cytochrome *b₆f* complex to structure changes in the hinge region of the Rieske iron−sulfur protein. *J. Biol. Chem. 278*, 20925–20933.

42. de Vitry, C., Ouyang, Y., Finazzi, G., Wollman, F. A., and Kallas, T. (2004) The chloroplast Rieske iron−sulfur protein. At the crossroad of electron transport and signal transduction. *J. Biol. Chem. 279*, 44621–44627.

43. Finazzi, G., Buschlen, S., de Vitry, C., Rappaport, F., Joliot, P., and Wollman, F. A. (1997) Function-directed mutagenesis of the cytochrome *b₆f* complex in *Chlamydomonas reinhardtii*: Involvement of the cd loop of cytochrome *b₆* in quinol binding to the Q_o site. *Biochemistry 36*, 2867–2874.

44. Zhang, Z., Huang, L., Shulmeister, V. M., Chi, Y. I., Kim, K. K., Hung, L. W., Crofts, A. R., Berry, E. A., and Kim, S. H. (1998) Electron transfer by domain movement in cytochrome *bc₁*. *Nature 392*, 677–684.

45. Breyton, C. (2001) Conformational changes in the cytochrome *b₆f* complex induced by inhibitor binding. *J. Biol. Chem. 275*, 13195–13201.